Tribology International 107 (2017) 56–64

Contents lists available at ScienceDirect

Tribology International

journal homepage: www.elsevier.com/locate/triboint

Anti-shock characteristics of water lubricated bearing for fuel cell vehicle air compressor

Tianming Ren, Ming Feng*

School of Mechanical Engineering, University of Science and Technology Beijing, Beijing 100083, China

ARTICLE INFO

Keywords:
Water lubrication
Lobe pocket bearing
Anti-shock characteristics
Fuel cell compressor

ABSTRACT

This paper presents an investigation of the anti-shock characteristics of water lubricated journal bearing used in the motorized centrifugal air compressor for fuel cell vehicles (FCV). The nonlinear trajectory of the shaft under a half sinusoidal shock load is numerically calculated by simultaneously solving the shaft motion equations and the Reynolds equation. Meanwhile, the pressure-compliance relationship of elastic-plastic roughness contact is also introduced to consider the possible direct contact between the spinning shaft and sleeve during shock. The influences of shock direction, amplitude, time and geometrical parameters on the anti-shock performance of the bearing are analyzed.

1. Introduction

The launch of TOYOTA MIRAI at the end of 2014 marks the FCV into the era of mass production. And consequently, the related technologies have entered a rapid development track. As the power source of such vehicle, the fuel cell system needs an air compressor to supply pressured oxygen for the stack. Comparing with the twin-screw compressor, the motorized centrifugal compressor is regarded to be an ideal solution for its high efficiency, low noise, long service span and compact in structure.

As one of the key technologies of the centrifugal compressor, the bearing is required to be oil-free and contaminant-free due to the sensitivity of the fuel cell proton exchange membrane. Therefore, the air lubricated compliant foil bearings were adopted by some makers [1–4]. Meanwhile, the authors demonstrated the possibility and merits of applying water lubricated hydro-static and -dynamic hybrid bearing in the compressor [5,6].

In general, shocks from moving car are inevitable, which may damage the compressor bearings due to the possible direct collision between the spinning shaft and sleeve. San Andrés and Ryu conducted a series of test on the conventional air bearings used in microturbomachinery [7–9]. In their experiments, the shock margin is about 30 G. However, the shock amplitude acting upon the compressor on a moving car can reach up to 50 G or more, which brings the margin concerns about the shock amplitude when using the air foil bearing.

Comparing with the air lubricated bearing, the water lubricated bearing possesses much higher load capacity and favorable stability while not increasing in power consumption [6]. Recent studies on the water lubricated bearing include the effects of the misalignment, local wear and particles on the load capacity [10–12], the thermal characteristics with different bush materials [13], and the dynamic performance in the application of high speed spindle [14], etc. However, up to now little knowledge we have about the anti-shock performance of the water lubricated bearing, especially in the case of the FCV application. A water lubricated hydro-static and -dynamic hybrid bearing with two lobe pockets is proposed in this paper and its anti-shock characteristics are clarified. The influences of shock direction, amplitude, time and geometrical parameters on the anti-shock performance are analyzed.

2. Bearing configuration

To improve efficiency and decrease dimensions, the motorized centrifugal air compressor is required to operate at the speed as high as 10^5 rpm or more. Therefore, the stability of the rotor-bearing system is an important issue to the compressor design. Since the bearings with the lobe type profile are recommended by many researchers for their excellent stability [15–17], a water lubricated hydro-static and -dynamic hybrid bearing with the lobe pockets is proposed for the compressor prototype, as shown in Fig. 1. The bearing has two lobe shallow pockets, whose profile is defined by the Archimedes helix with the starting point locating at the pocket boundary of the lobe downstream (corresponding to the rotation direction). Lubricating water is supplied through the two orifices closing to the lobe circumferential boundary of the upstream to help improve lubrication characteristics and eliminate cavitation phenomenon. The axial lands at the two sides of the lobes are designed to improve the hydrostatic effects and reduce water flow quantity. The bearing parameters are listed in Table 1. The

* Corresponding author.

http://dx.doi.org/10.1016/j.triboint.2016.11.016
Received 2 September 2016; Received in revised form 30 October 2016; Accepted 3 November 2016
Available online 14 November 2016

Nomenclature

a_c	real contact area, μm^2
B	bearing width, mm
B_1	lobe axial width, mm
D	bearing diameter, mm
d	distance between rough surface mean plane to the opposing smooth surface, mm
d_0	orifice diameter, mm
E	Young's modulus, Gpa
E_1, E_2	Young's moduli of journal and bearing, Gpa
$E()$	expectancy operation
e	eccentricity of journal, mm
e_u	eccentricity of mass of journal, mm
F	shock load, N
G	gravitational acceleration, 9.8 m s^{-2}
G_θ	circumferential turbulence coefficient
G_Z	axial turbulence coefficient
G_S	shock amplitude, G
H_B	Brinell hardness, Gpa
h	film thickness, mm
h_0	bearing clearance, mm
h_p	lobe depth, mm
$\bar{h}_p$	dimensionless lobe depth
h_T	local bearing clearance, mm
K	hardness coefficient
m	mass of rotor, kg
N_s	number of asperities per unit area, mm^{-2}
p_c	contact pressure, Pa
p_h	hydrodynamic pressure, Pa
P_s	water supply pressure, Pa
R_s	average radius of asperity summits, μm
T_s	shock time, s
T_{Max}	terminal time in the calculation time, s
W	reaction force, N
X, Y, Z	coordinate axis
Y_S	yield strength of material, Y_S=H_B/2.8
γ_C	pocket circumferential width ratio
γ_a	pocket axial width ratio
δ	height of roughness, mm
Θ_Z	rotational angle of rotor, 1
$\dot{\Theta}_Z$	angular velocity of rotor, 1/s
$\ddot{\Theta}_Z$	angular acceleration of rotor, 1/s^2
θ	angular coordinate
θ_0	positional angle of lobe, /°
θ_1	angular width of lobe, /°
θ_S	shock angle, /°
θ_L	load angle, /°
μ	water dynamic viscosity, Pa s
ν	Poisson's ratio
σ	combined standard deviation of rough surfaces
σ_S	combined standard deviation of asperity heights
$\phi_{p\theta}$	circumferential pressure flow factor
ϕ_{pZ}	axial pressure flow factor
ψ	composite probability density function (PDF) of rough surface
ψ_S	composite PDF of asperity height
ω	interference, $\omega = \delta - d$
ω_p	critical interference of elastic deformation

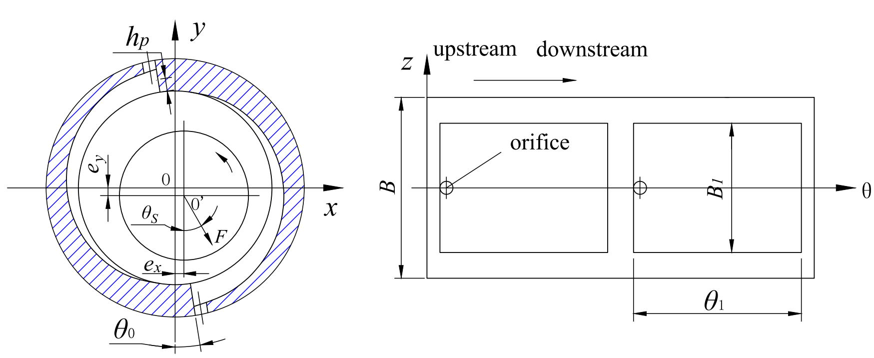

Fig. 1. Bearing configuration and the coordinate system.

Table 1
Parameters of the bearing.

Journal diameter D/mm	15
Bearing length B/mm	14
Radial clearance h_0/mm	0.02
Lobe depth h_p/mm	0.06
Lobe location angle θ_0/°	9
Lobe circumferential width θ_1/°	162
Pocket axial width B_1/mm	10
Orifice diameter d_0/mm	1.0
Water supply pressure P_S/Mpa	0.17
Viscosity of water μ/P_as	0.001
Nominal angular velocity of shaft $\dot{\Theta}_Z$/s^{-1}	1000π/3
Mass of shaft m/kg	0.28
Eccentricity of shaft mass e_u/μm	0.5

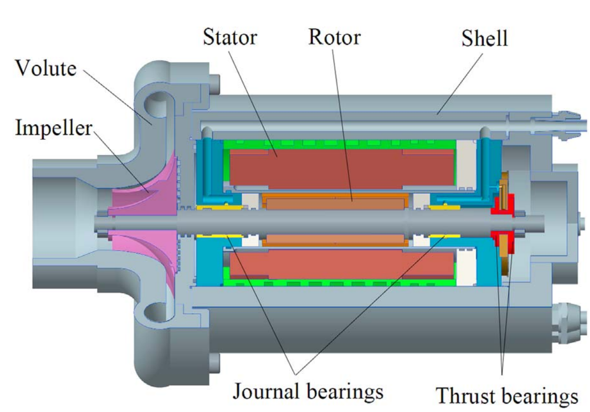

Fig. 2. Configuration of the compressor prototype.